

Improvement of nasal airway ventilation after rapid maxillary expansion evaluated with computational fluid dynamics

Tomonori Iwasaki,^a Issei Saitoh,^b Yoshihiko Takemoto,^c Emi Inada,^c Ryuzo Kanomi,^d Haruaki Hayasaki,^e and Youichi Yamasaki^f

Kagoshima, Himeji, and Niigata, Japan

Introduction: Rapid maxillary expansion is known to improve nasal airway ventilation. However, it is difficult to precisely evaluate this improvement with conventional methods. The purpose of this longitudinal study was to use computational fluid dynamics to estimate the effect of rapid maxillary expansion. **Methods:** Twenty-three subjects (9 boys, 14 girls; mean ages, 9.74 ± 1.29 years before rapid maxillary expansion and 10.87 ± 1.18 years after rapid maxillary expansion) who required rapid maxillary expansion as part of their orthodontic treatment had cone-beam computed tomography images taken before and after rapid maxillary expansion. The computed tomography data were used to reconstruct the 3-dimensional shape of the nasal cavity. Two measures of nasal airflow function (pressure and velocity) were simulated by using computational fluid dynamics. **Results:** The pressure after rapid maxillary expansion (80.55 Pa) was significantly lower than before rapid maxillary expansion (147.70 Pa), and the velocity after rapid maxillary expansion (9.63 m/sec) was slower than before rapid maxillary expansion (13.46 m/sec). **Conclusions:** Improvement of nasal airway ventilation by rapid maxillary expansion was detected by computational fluid dynamics. (Am J Orthod Dentofacial Orthop 2012;141:269-78)

Rapid maxillary expansion has been widely used by orthodontists to increase the maxillary transverse dimensions of young patients. Recent studies have suggested that rapid maxillary expansion also

increases nasal width and volume.¹⁻⁴ Therefore, rapid maxillary expansion has been generally considered to diminish the resistance of nasal airflow.⁵⁻⁸

Timms⁹ reported that 82% of patients had fewer upper respiratory infections after expansion. Gray¹⁰ reported that, after expansion, the incidences of colds, respiratory illnesses, allergic rhinitis, and asthma were reduced by half. Therefore, rapid maxillary expansion has been suggested as a treatment option for rhinostenosis caused by septal deformity, nasal infection, allergic rhinitis, and obstructive sleep apnea.⁹⁻¹² However, rapid maxillary expansion should not be encouraged as a treatment option for improvement of nasal airway ventilation conditions without an orthodontic indication.¹³

Previous methods of evaluating nasal airway ventilation include x-rays,³ computed tomography,^{14,15} rhinomanometry,^{16,17} and acoustic rhinometry.¹⁸⁻²⁰ However, it is difficult to take precise measurements of nasal airway ventilation with these methods because of the complicated form of the nasal airway lumen. Therefore, there is not enough evidence that nasal airway ventilation improves with rapid maxillary expansion.²¹

To better evaluate the relationship between respiratory function and nasal morphology, a 3-dimensional

^aLecturer, Developmental Medicine, Health Research Course, Graduate School of Medical and Dental Sciences, Kagoshima University, Kagoshima, Japan.

^bAssistant professor, Developmental Medicine, Health Research Course, Graduate School of Medical and Dental Sciences, Kagoshima University, Kagoshima, Japan.

^cResearch associate, Developmental Medicine, Health Research Course, Graduate School of Medical and Dental Sciences, Kagoshima University, Kagoshima, Japan.

^dPrivate practice, Himeji, Japan.

^eProfessor and chairman, Division of Pediatric Dentistry, Department of Oral Health Science, Course of Oral Life Science, Graduate School of Medical and Dental Sciences, Niigata University, Niigata, Japan.

^fProfessor and chairman, Developmental Medicine, Health Research Course, Graduate School of Medical and Dental Sciences, Kagoshima University, Kagoshima, Japan.

The first author invented fluid-mechanical simulation; Kagoshima University holds the know-how, and specific licences are assigned the right to manufacture and distribute it. The other authors report no commercial, proprietary, or financial interest in the products or companies described in this article.

Supported by KAKENHI from the Japan Society for the Promotion of Science (numbers 19592360 and 22592292).

Reprint requests to: Tomonori Iwasaki, Field of Developmental Medicine, Health Research Course, Graduate School of Medical and Dental Sciences, Kagoshima University, 8-35-1, Sakuragaoka Kagoshima-City, Kagoshima, 890-8544, Japan; e-mail, yamame@dent.kagoshima-u.ac.jp.

Submitted, February 2011; revised and accepted, August 2011.

0889-5406/\$36.00

Copyright © 2012 by the American Association of Orthodontists.

doi:10.1016/j.ajodo.2011.08.025

(3D) model of each subject's nasal cavity was constructed from computed tomography data and used to create computational fluid dynamics models of respiratory status during quiet respiration.²² Unlike some conventional methods that cannot separate nasal airflow from nasopharyngeal airflow, computational fluid dynamics can evaluate airflow in the nasal cavity alone, giving a more accurate evaluation of the effect of rapid maxillary expansion. The purpose of this study was to use computational fluid dynamics to more precisely evaluate and clarify the amount of the nasal airway ventilation improvement after rapid maxillary expansion.

MATERIAL AND METHODS

A total of 23 patients, who visited the Kanomi Orthodontic Office (Himeji, Japan) for orthodontic treatment, participated in this longitudinal study (9 boys, 14 girls). Their mean ages before and after rapid maxillary expansion treatment were 9.74 ± 1.29 years and 10.87 ± 1.18 years, respectively. They included 10 patients with paranasal mucosa hyperplasia, 1 with adenoid tonsillar hypertrophy, and 3 with tonsillar hypertrophy. None of these subjects received surgical treatment for these conditions during the rapid maxillary expansion treatment.

All patients in this study required approximately 5 mm of maxillary expansion as part of their orthodontic treatment. Those who had previous orthodontic treatment or craniofacial or growth abnormalities were excluded. The study was reviewed and approved by the Ethics Committee of the Kagoshima University Graduate School of Medical and Dental Sciences, Kagoshima, Japan.

Each subject was seated in a chair with his or her Frankfort horizontal plane parallel to the floor. A cone-beam computed tomography scanner (CB MercuRay, Hitachi Medical, Tokyo, Japan) was set to maximum 120 kV, maximum 15 mA, and exposure time of 9.6 seconds. No subject had used a nasal decongestant at the time of the cone-beam computed tomography scan. The data were sent directly to a personal computer and stored in digital imaging and communications in medicine format.

For the evaluation of nasal and intermaxillary molar widths, a 3D coordinate system and 3D images were constructed with a medical image analyzing system (ImagnosisVE, Imagnosis, Kobe, Japan).²³ From the 3D reconstructed images, the 3D nasal width (distance between the most lateral points of the nasal cavity) and the intermaxillary molar width (distance between the most medial points of the constricted part of the maxillary first molars) were measured to evaluate the changes produced by rapid maxillary expansion (Figs 1 and 2).

For the evaluation of the nasal airway ventilation condition, morphologic evaluation, volume-rendering software (INTAGE Volume Editor, CYBERNET, Tokyo, Japan) was used to create the 3D volume data of the nasal cavity. To construct an anatomically correct 3D model of each subject's nasal cavity, approximately 150 slices from a computed tomography image were used. The images were obtained at intervals of 0.377 mm from the frontal sinus to the inferior nasal meatus. Because the nasal airway is a void surrounded by hard and soft tissues, inversion of the 3D-rendered image is required, converting a negative value to a positive value and vice versa. Threshold segmentation was used to select the computed tomography units in the nasal airway. Because the inverted air space has a significantly greater positive computed tomography unit than the denser surrounding soft tissue, the distinct high-contrast border produces clean segmentation of the nasal airway. By modifying the threshold limits, an appropriate range defined the tissues of interest in the volume of interest for a particular scan. By using this concept, a threshold of computed tomography units was selected to isolate all empty spaces in the nasal airway region, which also included other cavities such as the paranasal sinuses.²⁴ Subsequently, by using an appropriate smoothing algorithm with a moving average, the 3D model was converted to a smooth model without losing the patient-specific character of the upper airway shape.²⁵ The rendered volume data were in a 512×512 matrix with a voxel size of 0.377 mm. Examples of the 3D form of extracted nasal cavities (from the external nares to internal nares) and the paranasal sinuses are shown in Figure 3. When the continuity of the bilateral nasal meatus was broken, a complete obstruction was assumed (Fig 3, A).

For the functional evaluation, computational fluid dynamics were used to estimate the airflow pattern of just the nasal airway (Fig 4).²² The constructed 3D images for the nasal airway were exported to fluid-dynamic software (PHOENICS, CHAM-Japan, Tokyo, Japan) in stereolithographic format. This software can simulate and evaluate various kinds of computational fluid dynamics under a set of given conditions. In our simulation, air flowed from the choana horizontally, and air was exhaled through both nostrils. The flow was assumed to be a Newtonian, homogeneous, and incompressible fluid.²⁶ Elliptic-staggered equations and the continuity equation were used in the study.²⁷ The computational fluid dynamics of the nasal airway were performed under the following conditions by using PHOENICS: (1) the volume of air flowed with a velocity of 200 mL per second,²⁸ (2) the wall surface was nonslip, and (3) the simulation was repeated 1000 times to

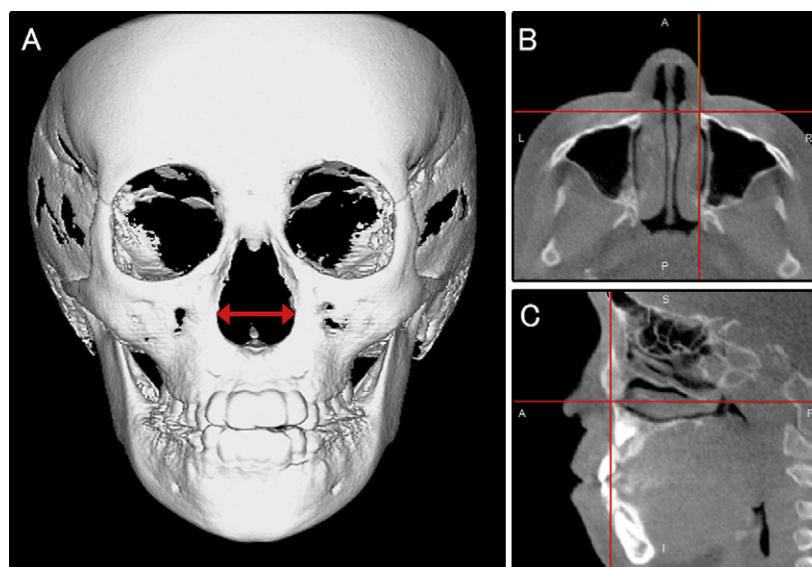


Fig 1. Measurement of 3D nasal width: **A**, locating the widest portion of the nasal aperture in a 3D computed tomography reconstruction to set the measurement points in the **B**, coronal and **C**, sagittal section images.

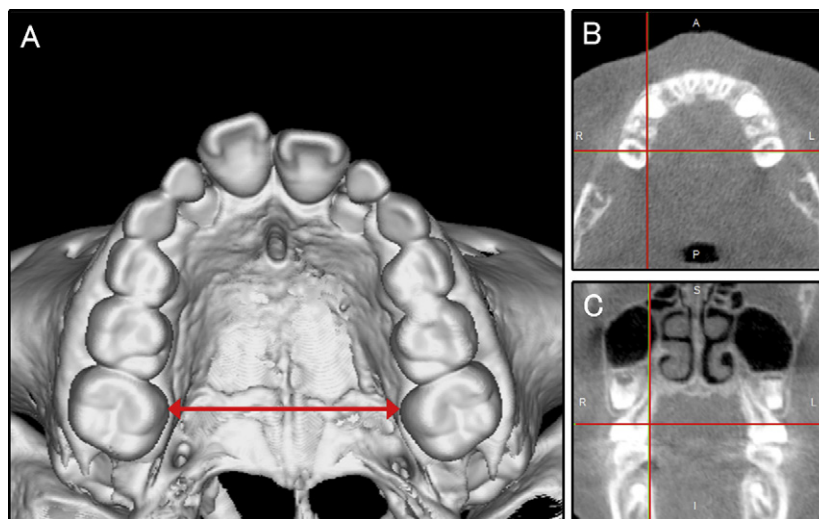


Fig 2. Measurement of 3D intermaxillary molar width: **A**, locating the intermaxillary molar width at the narrowest portion in a 3D computed tomography reconstruction to set the measurement points in the **B**, horizontal and **C**, coronal section images.

calculate the mean values. Convergence was judged by monitoring the magnitude of the treatment residual sources of mass and momentum, normalized by the respective inlet fluxes. The iteration was continued until all residuals fell below 0.2%.

The simulation estimated airflow pressure and velocity. In subjects whose 3D morphologic evaluation indicated a nasal airway obstruction, computational fluid

dynamics were not performed. When computational fluid dynamics indicated a maximum pressure of more than 100 Pa (with an inflow rate of 200 mL/sec) and a maximum velocity of more than 10 m per second, an obstruction was assumed in that subject.²²

The patients were classified into 3 groups by their ventilation conditions both before and after rapid maxillary expansion: (1) those in whom an obstruction was

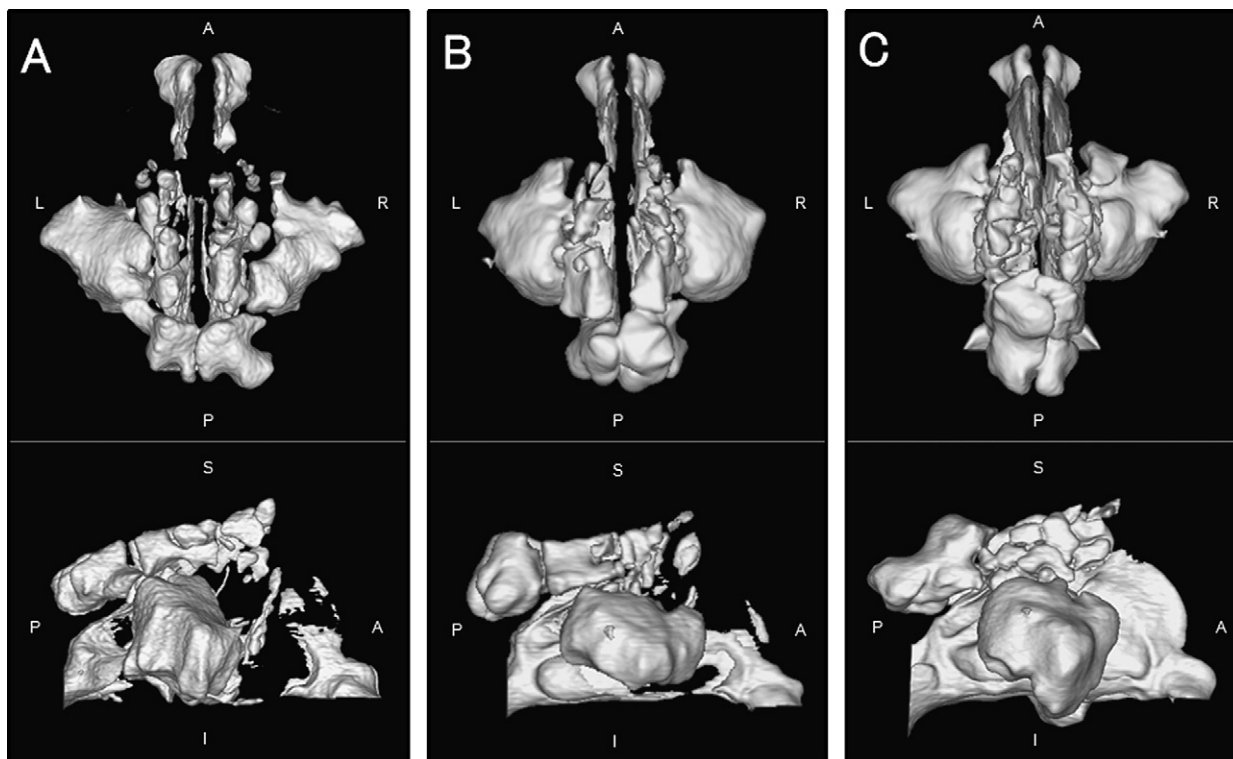


Fig 3. Evaluation of nasal airway obstruction from the 3D nasal cavity forms in 3 subjects (*top image*, superior view; *bottom image*, lateral view): **A**, obvious complete obstruction; **B**, rhinostenosis, but the presence or absence of complete obstruction cannot be determined; **C**, no rhinostenosis or obstruction.

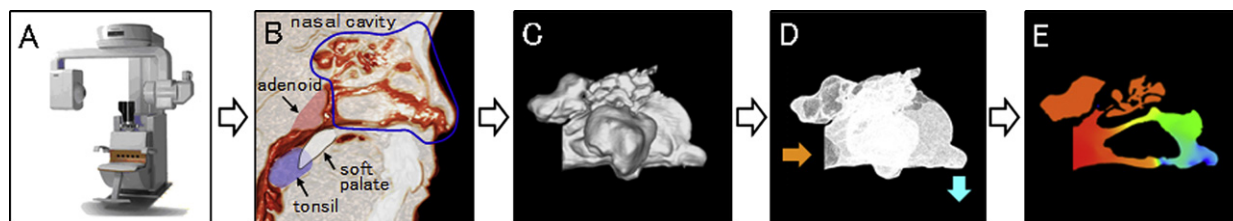


Fig 4. Steps in the evaluation of nasal cavity ventilation by computational fluid dynamics: **A**, cone-beam computed tomography instrument; **B**, extraction of the nasal cavity data; **C**, volume rendering and smoothing; **D**, construction of the stereolithographic model and numeric simulation; **E**, evaluation of the nasal cavity ventilation condition.

detected in the 3D morphologic evaluation, (2) those in whom an obstruction was detected with computational fluid dynamics but not with the 3D morphologic evaluation, and (3) those in whom no obstruction was detected with either method (Fig 5).

Statistical analysis

A paired *t* test was used to compare both the nasal and the intermaxillary molar widths before and after rapid maxillary expansion. The Mann-Whitney U test was used to compare nasal airway ventilation conditions

before and after rapid maxillary expansion. Spearman correlation coefficients were calculated to evaluate the relationships between transverse dimensions and nasal airway ventilation conditions. The McNemar test was used to clarify the improvement of obstruction before and after rapid maxillary expansion. Statistical significance was set at *P* < 0.05.

To assess the measurement error, 10 randomly selected computed tomography images from among the 46 had the nasal and intermaxillary molar widths measured twice by the same operator (T.I.) in 1 week.

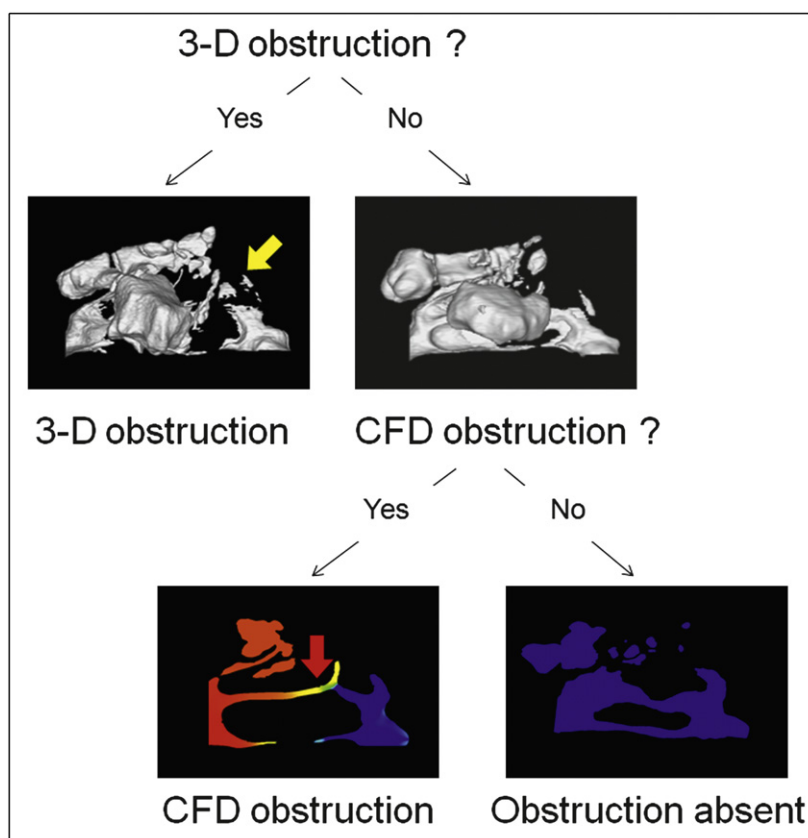


Fig 5. Three conditions (3D obstruction, computational fluid dynamics obstruction, and no obstruction) of the nasal airway with 3D models and computational fluid dynamics. (yellow arrow, 3D obstruction; red arrow, computational fluid dynamics obstruction). *CFD*, Computational fluid dynamics.

Table I. Changes of nasal and intermaxillary molar widths before and after rapid maxillary expansion

	Before RME (n = 23)		After RME (n = 23)		Paired t test
	Mean	SD	Mean	SD	P
Nasal width (mm)	21.39	1.51	23.48	1.83	<0.001
Intermaxillary molar width (mm)	32.18	2.42	36.07	2.74	<0.001

RME, Rapid maxillary expansion.

A paired *t* test detected no statistically significant differences. Dahlberg’s error of method (double determination method) was computed, and the results were 0.055 mm for nasal width and 0.072 mm for intermaxillary molar width.²⁹ According to all repeated analyses, the method error was considered negligible.

RESULTS

Nasal width after rapid maxillary expansion (23.48 ± 1.83 mm) was significantly greater than before

rapid maxillary expansion (21.39 ± 1.51 mm) (Table I). Figure 6 shows a typical subject before and after rapid maxillary expansion. Intermaxillary molar width after rapid maxillary expansion (36.07 ± 2.74 mm) was also significantly greater than before rapid maxillary expansion (32.18 ± 2.42 mm) (Table I).

Before rapid maxillary expansion, 18 of the 23 patients (78%) had an obstruction detected by either 3D reconstruction or computational fluid dynamics. After rapid maxillary expansion, only 6 patients (26%) had a detectable obstruction (Table II). The change in the number of patients with obstruction after rapid maxillary expansion was statistically significant according to the McNemar test (Table II). A typical patient whose nasal airway ventilation improved after rapid maxillary expansion is shown in Figure 7. Twelve of the 18 patients (66.7%) who had an obstruction before rapid maxillary expansion had no obstruction after rapid maxillary expansion.

Among the 22 patients without a morphologic obstruction, the pressure after rapid maxillary expansion (80.55 ± 76.59 Pa) was significantly lower in 18 of them

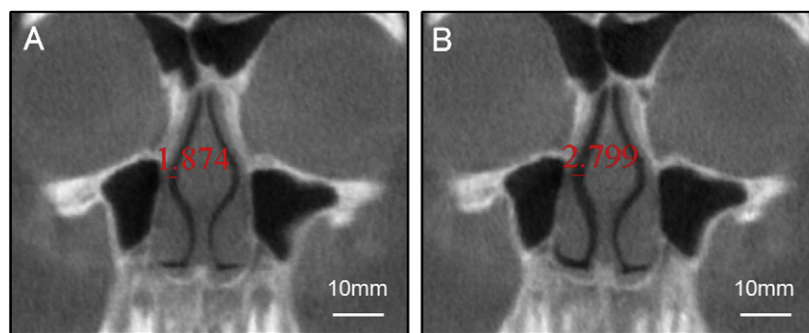


Fig 6. Cone-beam computed tomography images of a patient with a nasal width expansion of 2 mm (A, before rapid maxillary expansion; B, after rapid maxillary expansion): **A**, the greatest width of the nasal cavity was comparatively narrow; **B**, the greatest width of the nasal cavity was expanded approximately 1 mm. This was enough expansion of nasal cavity area; however, evaluation of nasal airway ventilation improvement was difficult with the morphologic data alone.

than before rapid maxillary expansion (147.70 ± 94.87 Pa). Similarly, the velocity in these 22 patients after rapid maxillary expansion (9.63 ± 6.67 m/sec) was significantly lower in 18 than before rapid maxillary expansion (13.46 ± 5.99 m/sec).

Table III shows the correlations between transverse dimensions and ventilation conditions. Before rapid maxillary expansion, the transverse dimension was not significantly correlated with the ventilation condition. After rapid maxillary expansion, the transverse dimension was negatively correlated with the ventilation condition, and the intermaxillary molar width showed the only significant negative correlation with maximum pressure. The treatment change in the transverse dimension was not significantly correlated with the treatment change in ventilation condition.

DISCUSSION

The main purpose of this study was to precisely evaluate the improvement of nasal airway obstruction by rapid maxillary expansion by using computational fluid dynamics. Many studies have found that rapid maxillary expansion improves nasal airway ventilation.^{6,7,21,30-33} However, the extreme complexity of the nasal airway form makes reliable evaluation of the ventilation condition difficult, and it has not been possible to establish the improvement after rapid maxillary expansion. Because computational fluid dynamics can evaluate the ventilation condition in the nasal cavity in isolation from the nasopharynx, a more accurate assessment of changes induced by rapid maxillary expansion is possible.²²

Christie et al³⁴ concluded, in their cone-beam computed tomography study, that nasal cavity width increases significantly (2.73 mm) after rapid maxillary

expansion. Their rapid maxillary expansion of 8.19 mm was greater than in our study (approximately 5 mm), and their reported increase in nasal cavity width was correspondingly greater than ours (2.09 mm) (Table I). We confirmed previous reports that the transverse increase at the level of the nasal floor corresponds to one third of the amount of rapid maxillary expansion.^{34,35} Based on reconstructed computed tomography models, clinically significant long-term maxillary molar width increases of 3.7 to 4.8 mm can be achieved with rapid maxillary expansion.³⁶ This increase in intermaxillary molar width (3.89 mm) was slightly smaller than that reported by Lagravère et al.³⁶ Because this expansion was smaller in this study than conventional expansion (ie, 5-10 mm), it was expected that the improvement of the ventilation condition would also be less.

Functional evaluation of nasal airway ventilation improvement after rapid maxillary expansion requires measurement of nasal cavity airflow alone. Because the nasal cavity has a complicated lumen, evaluation of the nasal airway is extremely difficult with morphologic data alone. One must evaluate not only the cross-sectional area but also the cross-sectional form and the continuity of the lumen. Because computational fluid dynamics simulate the magnitudes of air pressure and velocity, the function of the entire nasal airway can be evaluated more precisely than would be possible with morphologic evaluation alone.

Xiong et al,³⁷ in a computational fluid dynamics study, reported an increased distribution of paranasal airflow after functional endoscopic sinus surgery, and that nasal airway resistance decreased. Paranasal mucosa hyperplasia was observed in half of our subjects. Therefore, we included the paranasal sinuses in our computational fluid dynamics to reflect it.

Table II. Changes of ventilation conditions before and after rapid maxillary expansion

Patient	Before RME			After RME			Ventilation improvement	Palatal expansion (mm)*
	Ventilation condition	Maximum pressure (Pa)	Maximum velocity (m/sec)	Ventilation condition	Maximum pressure (Pa)	Maximum velocity (m/sec)		
1	× 3D	-	-	× CFD	320.8	29.0	No	2.87
2	× CFD	131.5	14.0	○	9.9	2.2	Yes	4.70
3	○	76.4	11.0	○	67.5	8.7	-	3.06
4	○	56.7	14.3	○	7.8	2.4	-	3.04
5	× CFD	335.2	15.4	○	68.4	8.4	Yes	3.96
6	× 3D	-	-	○	75.5	9.9	Yes	4.04
7	× CFD	158.8	11.5	× CFD	118.8	12.7	No	3.15
8	× 3D	-	-	○	30.7	8.1	Yes	4.54
9	× CFD	117.9	10.4	○	35.2	7.1	Yes	5.05
10	× CFD	186.0	14.1	× CFD	197.8	18.0	No	2.78
11	× CFD	156.6	15.4	○	53.4	5.3	Yes	4.93
12	○	25.8	5.4	○	27.7	3.7	-	4.81
13	× CFD	327.7	18.8	○	64.4	10.7	Yes	5.45
14	○	69.9	8.1	○	30.2	7.5	-	4.21
15	× CFD	107.4	13.3	○	59.1	10.9	Yes	4.54
16	× CFD	106.3	11.4	○	63.8	8.1	Yes	3.14
17	× CFD	250.2	23.2	× CFD	175.9	18.1	No	2.40
18	× CFD	130.5	12.2	○	49.6	3.7	Yes	5.02
19	× CFD	105.1	12.0	○	43.6	3.4	Yes	3.52
20	× 3D	-	-	× 3D	-	-	No	3.02
21	○	31.5	2.8	○	8.8	2.9	-	4.48
22	× 3D	-	-	○	75.6	11.6	Yes	4.03
23	× CFD	285.2	29.1	× CFD	187.6	19.8	No	2.69
Mean		147.70	13.46		80.55	9.63		3.89
SD		94.87	5.99		76.59	6.67		0.91
P		0.008 [†]	0.017 [†]					
No obstruction	5			17				
Obstruction	18			6				
Improvement ratio							66.7% (12/18) [‡]	

RME, Rapid maxillary expansion; ○, no obstruction; ×, obstruction; 3D, morphologic complete obstruction; CFD, obstruction detected only in computational fluid dynamics.

*Change of intermaxillary molar width; [†]Statistically significant at $P < 0.05$ vs after RME; [‡]McNemar test: $P < 0.001$.

Figure 3 shows representative examples of 3 types of 3D form before rapid maxillary expansion. In one, complete obstruction of the nasal cavity (Fig 3, A) is easily observed. In a more difficult case (Fig 3, B), it is not possible to determine the presence of an obstruction from the 3D form. Nevertheless, a nasal airway obstruction was detected by computational fluid dynamics (Fig 5). These 2 subjects illustrate how the nasal airway ventilation condition can be evaluated more precisely with computational fluid dynamics, regardless of the complexity of the form.

With computed tomography images, no discontinuity of the nasal cavity image was seen in 18 children before rapid maxillary expansion and in 22 children after rapid maxillary expansion. However, with computational fluid dynamics, only 5 children had no obstruction before rapid maxillary expansion and only 12 after rapid

maxillary expansion (Table II). In other words, the incidence of detected functional obstruction was much higher with computational fluid dynamics.

By using a conventional method, it was reported that rapid maxillary expansion decreases 45% to 61.3% of the incidence of nasal airway obstruction.^{6,21,31}

Crouse et al³⁸ reported that nasal airway resistance in 9- to 10-year-old normal children ranged from 3.0 to 5.0 cm of water per liter per second. So, in this study, airway-resistance values of more than 5.0 cm of water per liter per second were considered to indicate obstruction with 100 Pa of pressure at an inflow of 200 mL per second.²² However, these criteria for obstruction are arbitrary. Other thresholds could produce different results. Still, our study with computational fluid dynamics might have found a higher incidence of nasal obstruction before and after rapid maxillary expansion, and reduction

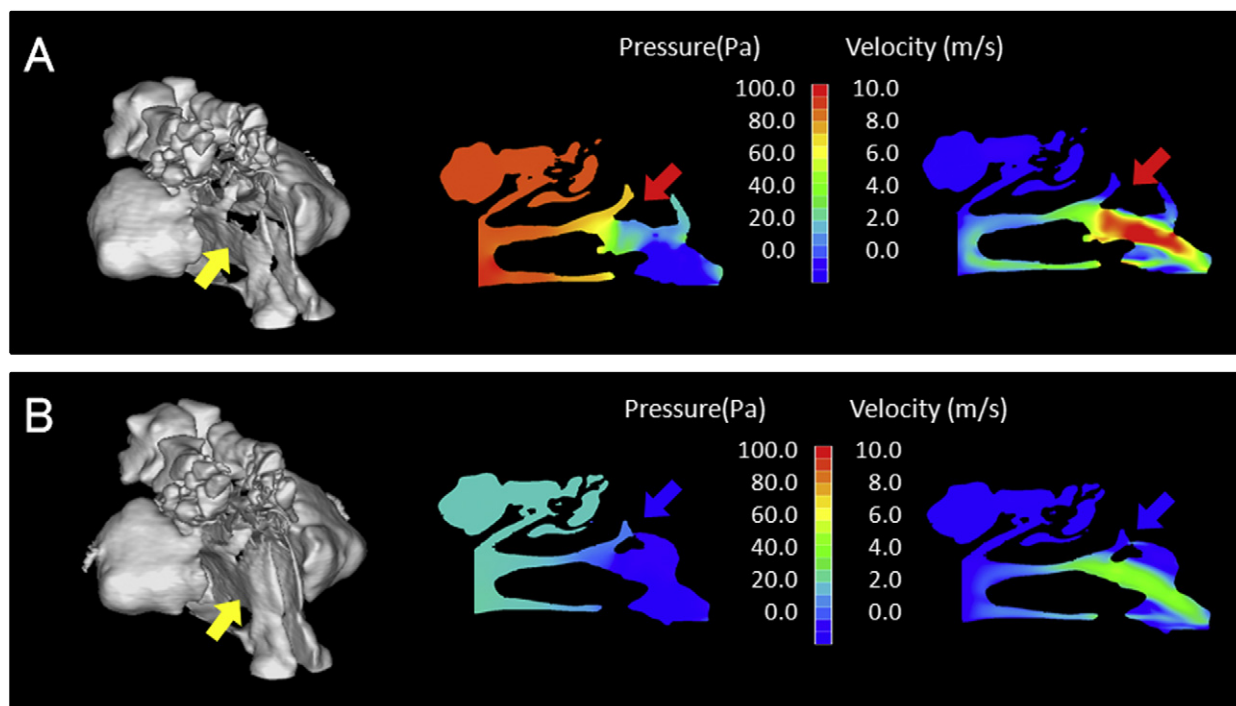


Fig 7. Example of change in the ventilation condition after rapid maxillary expansion in a patient (**A**, before rapid maxillary expansion; **B**, after rapid maxillary expansion): **A**, stenosis of the nasal cavity can be seen, but the presence of an obstruction cannot be determined from the 3D form (*yellow arrow*); nevertheless, computational fluid dynamics shows that the maximum pressure and maximum velocity were both high (*red arrow*), indicating an obstruction. **B**, The 3D form indicates improvement of the stenosis, but it cannot determine whether the obstruction was reduced (*yellow arrow*). On the other hand, computational fluid dynamics show that both pressure and velocity decreased (*blue arrow*), and the obstruction was reduced.

of nasal airway obstruction in 66.7% of the patients. According to our 3D computed tomography images, 5 patients had an obstruction before rapid maxillary expansion, but only 1 patient after rapid maxillary expansion had an obstruction (Table II). This is an improvement rate of 80%. However, the improvement rate with 3D computed tomography images and computational fluid dynamics (66.7%) was lower than that of 3D computed tomography images alone (80.0%). This is because computational fluid dynamics, which can account for the complicated shape of the nasal airway, are more sensitive to nasal airway obstructions both before and after rapid maxillary expansion.

Computational fluid dynamics can evaluate the ventilation conditions in the nasal cavity alone, without the effects of the adenoids, palatine tonsils, and soft palate. Moreover, it is possible to identify any obstruction of the nasal airway by using computational fluid dynamics with a 3D model of the morphology.

Previously reported decreases in nasal airway resistance after rapid maxillary expansion range from

33%³⁹ to 45%⁶ measured by rhinomanometry, and from 31.6%³¹ to 35.0%²¹ measured by acoustic rhinometry. Using computational fluid dynamics, we found a decrease of 46.5% for pressure. This decrease in nasal airway resistance was greater than in previous reports. Because different methods were used, a precise comparison was not possible, but computational fluid dynamics might have detected improvements of nasal airway ventilation more precisely after rapid maxillary expansion.

Kobayashi et al⁴⁰ reported normal nasal airway resistance of fourth grade elementary school children (approximately 10 years old) to be 0.38 Pa per cubic centimeter per second. This resistance value was considered 76 Pa of pressure at in flow of 200 mL per second. Also, they reported that the resistance value of the children with nasal airway obstruction was 0.57 Pa per cubic centimeter per second (114 Pa). We found a somewhat higher pressure with nasal airway obstruction before rapid maxillary expansion (147.70 Pa) and a somewhat lower pressure after rapid maxillary expansion (80.55 Pa) than did Kobayashi et al.

Table III. Spearman rank correlation coefficients and *P* values (in parentheses) between transverse dimension and ventilation condition

	<i>Before RME</i>		<i>After RME</i>		<i>Absolute change</i>	
	<i>Maximum pressure</i>	<i>Maximum velocity</i>	<i>Maximum pressure</i>	<i>Maximum velocity</i>	<i>Maximum pressure</i>	<i>Maximum velocity</i>
Before RME						
Nasal width	0.046 (0.855)	0.017 (0.948)	-	-	-	-
Intermaxillary molar width	-0.350 (0.155)	-0.186 (0.460)	-	-	-	-
After RME						
Nasal width	-	-	-0.302 (0.173)	-0.242 (0.278)	-	-
Intermaxillary molar width	-	-	-0.458 (0.032)*	-0.344 (0.177)	-	-
Absolute change						
Nasal width	-	-	-	-	-0.215 (0.397)	0.096 (0.710)
Intermaxillary molar width	-	-	-	-	-0.340 (0.168)	-0.121 (0.633)

RME, Rapid maxillary expansion.

*Statistically significant at $P < 0.05$.

Because nasal airway resistance is variable for some time after rapid maxillary expansion, measurement of the effect of rapid maxillary expansion on nasal airway ventilation should be taken several months later.^{6,7,9,10} Our posttreatment computed tomography data were taken more than 7 months after rapid maxillary expansion and after 4 months of retention, when nasal airway ventilation should be stable.⁴¹

Palatal expansion influenced nasal airway resistance (Table II). However, the amount of expansion did not show a clear relationship between transverse dimension and nasal airway resistance (Table III). There were great individual differences in ventilation conditions before rapid maxillary expansion (Table II). Furthermore, individual differences in nasal cavity shape and nasal mucosa thickness are thought to be large. For these reasons, a clear relationship might not be shown between transverse dimension and nasal airway resistance.

One limitation of our study was that nasal airway ventilation can also be influenced by growth changes.⁴² Ideally, an age-matched control sample should have been compared with the rapid maxillary expansion patients. For the age range in our study, the reported growth-related decrease in nasal airway resistance was only 0.1 cm of water per liter per second per year (5 Pa).⁴² Because this change is only about 7% of the change observed with rapid maxillary expansion, we concluded that expansion was responsible for most of the change.

In addition, we had no clinically measured airflow resistance in our subjects to compare with their airflow resistance determined by computational fluid dynamics. In the future, we intend to compare our subjects' clinical examination data, such as polysomnography and

rhinomanometry, with computational fluid dynamics analysis of their airflow resistance of the nasal cavity.

CONCLUSIONS

Because computational fluid dynamics can evaluate airflow in the nasal cavity alone, it might give a more accurate evaluation of the effect of rapid maxillary expansion. Therefore, computational fluid dynamics might be a more useful method for evaluating the ventilation condition of the nasal airway than conventional methods.

We thank Gaylord Throckmorton for reviewing this article for English usage.

REFERENCES

1. Cross DL, McDonald JP. Effect of rapid maxillary expansion on skeletal, dental, and nasal structures: a postero-anterior cephalometric study. *Eur J Orthod* 2000;22:519-28.
2. Chung CH, Font B. Skeletal and dental changes in the sagittal, vertical, and transverse dimensions after rapid palatal expansion. *Am J Orthod Dentofacial Orthop* 2004;126:569-75.
3. Basciftci FA, Mutlu N, Karaman AI, Malkoc S, Kucukkolbasi H. Does the timing and method of rapid maxillary expansion have an effect on the changes in nasal dimensions? *Angle Orthod* 2002;72:118-23.
4. Haralambidis A, Ari-Demirkaya A, Acar A, Kucukkes N, Ates M, Ozkaya S. Morphologic changes of the nasal cavity induced by rapid maxillary expansion: a study on 3-dimensional computed tomography models. *Am J Orthod Dentofacial Orthop* 2009;136:815-21.
5. Wertz RA. Changes in nasal airflow incident to rapid maxillary expansion. *Angle Orthod* 1968;38:1-11.
6. Hershey HG, Stewart BL, Warren DW. Changes in nasal airway resistance associated with rapid maxillary expansion. *Am J Orthod* 1976;69:274-84.

7. Hartgerink DV, Vig PS, Abbott DW. The effect of rapid maxillary expansion on nasal airway resistance. *Am J Orthod Dentofacial Orthop* 1987;92:381-9.
8. Compadretti GC, Tasca I, Bonetti GA. Nasal airway measurements in children treated by rapid maxillary expansion. *Am J Rhinol* 2006;20:385-93.
9. Timms DJ. Rapid maxillary expansion in the treatment of nasal obstruction and respiratory disease. *Ear Nose Throat J* 1987;66:242-7.
10. Gray LP. Results of 310 cases of rapid maxillary expansion selected for medical reasons. *J Laryngol Otol* 1975;89:601-14.
11. Timms DJ. Some medical aspects of rapid maxillary expansion. *Br J Orthod* 1974;1:127-32.
12. Gray LP. Rapid maxillary expansion and impaired nasal respiration. *Ear Nose Throat J* 1987;66:248-51.
13. Andre RF, Vuyk HD, Ahmed A, Graamans K, Nolst Trenite GJ. Correlation between subjective and objective evaluation of the nasal airway. A systematic review of the highest level of evidence. *Clin Otolaryngol* 2009;34:518-25.
14. Doruk C, Sokucu O, Bicakci AA, Yilmaz U, Tas F. Comparison of nasal volume changes during rapid maxillary expansion using acoustic rhinometry and computed tomography. *Eur J Orthod* 2007;29:251-5.
15. Palaia J, Ngan P, Martin C, Razmus T. Use of conventional tomography to evaluate changes in the nasal cavity with rapid palatal expansion. *Am J Orthod Dentofacial Orthop* 2007;132:458-66.
16. Clarke RW, Jones AS. The limitations of peak nasal flow measurement. *Clin Otolaryngol Allied Sci* 1994;19:502-4.
17. Jones AS, Lancer JM. Rhinomanometry. *Clin Otolaryngol Allied Sci* 1987;12:233-6.
18. Cakmak O, Coskun M, Celik H, Buyuklu F, Ozluoglu LN. Value of acoustic rhinometry for measuring nasal valve area. *Laryngoscope* 2003;113:295-302.
19. Cakmak O, Tarhan E, Coskun M, Cankurtaran M, Celik H. Acoustic rhinometry: accuracy and ability to detect changes in passage area at different locations in the nasal cavity. *Ann Otol Rhinol Laryngol* 2005;114:949-57.
20. Tomkinson A, Eccles R. Acoustic rhinometry: an explanation of some common artefacts associated with nasal decongestion. *Clin Otolaryngol Allied Sci* 1998;23:20-6.
21. Doruk C, Sokucu O, Sezer H, Canbay EI. Evaluation of nasal airway resistance during rapid maxillary expansion using acoustic rhinometry. *Eur J Orthod* 2004;26:397-401.
22. Iwasaki T, Saitoh I, Takemoto Y, Inada E, Kanomi R, Hayasaki H, et al. Evaluation of upper airway obstruction in Class II children with fluid-mechanical simulation. *Am J Orthod Dentofacial Orthop* 2011;139:e135-45.
23. Iwasaki T, Hayasaki H, Takemoto Y, Kanomi R, Yamasaki Y. Oropharyngeal airway in children with Class III malocclusion evaluated by cone-beam computed tomography. *Am J Orthod Dentofacial Orthop* 2009;136:318:e311-9; discussion 318-9.
24. Tso HH, Lee JS, Huang JC, Maki K, Hatcher D, Miller AJ. Evaluation of the human airway using cone-beam computerized tomography. *Oral Surg Oral Med Oral Pathol Oral Radiol Endod* 2009;108:768-76.
25. Kim YJ, Hong JS, Hwang YI, Park YH. Three-dimensional analysis of pharyngeal airway in preadolescent children with different anteroposterior skeletal patterns. *Am J Orthod Dentofacial Orthop*; 137:306.e301-11; discussion 306-7.
26. De Backer JW, Vanderveken OM, Vos WG, Devolder A, Verhulst SL, Verbracken JA, et al. Functional imaging using computational fluid dynamics to predict treatment success of mandibular advancement devices in sleep-disordered breathing. *J Biomech* 2007;40:3708-14.
27. Gamiño B, Aguillón J. Numerical simulation of syngas combustion with a multi-spark ignition system in a diesel engine adapted to work at the Otto cycle. *Fuel* 2010;89:581-91.
28. Xu C, Sin S, McDonough JM, Udupa JK, Guez A, Arens R, et al. Computational fluid dynamics modeling of the upper airway of children with obstructive sleep apnea syndrome in steady flow. *J Biomech* 2006;39:2043-54.
29. Dahlberg G. *Statistical methods for medical and biological students*. New York: Interscience Publications; 1940.
30. Monini S, Malagola C, Villa MP, Tripodi C, Tarentini S, Malagnino I, et al. Rapid maxillary expansion for the treatment of nasal obstruction in children younger than 12 years. *Arch Otolaryngol Head Neck Surg* 2009;135:22-7.
31. Oliveira De Felipe NL, Da Silveira AC, Viana G, Kusnoto B, Smith B, Evans CA. Relationship between rapid maxillary expansion and nasal cavity size and airway resistance: short- and long-term effects. *Am J Orthod Dentofacial Orthop* 2008;134:370-82.
32. De Felipe NL, Bhushan N, Da Silveira AC, Viana G, Smith B. Long-term effects of orthodontic therapy on the maxillary dental arch and nasal cavity. *Am J Orthod Dentofacial Orthop* 2009;136:490:e491-8; discussion 490-1.
33. Sokucu O, Doruk C, Uysal OI. Comparison of the effects of RME and fan-type RME on nasal airway by using acoustic rhinometry. *Angle Orthod* 2010;80:870-5.
34. Christie KF, Boucher N, Chung CH. Effects of bonded rapid palatal expansion on the transverse dimensions of the maxilla: a cone-beam computed tomography study. *Am J Orthod Dentofacial Orthop* 2010;137(Suppl):S79-85.
35. Garib DG, Henriques JF, Janson G, Freitas MR, Coelho RA. Rapid maxillary expansion—tooth tissue-borne versus tooth-borne expanders: a computed tomography evaluation of dentoskeletal effects. *Angle Orthod* 2005;75:548-57.
36. Lagravère MO, Major PW, Flores-Mir C. Long-term dental arch changes after rapid maxillary expansion treatment: a systematic review. *Angle Orthod* 2005;75:155-61.
37. Xiong G, Zhan J, Zuo K, Li J, Rong L, Xu G. Numerical flow simulation in the post-endoscopic sinus surgery nasal cavity. *Med Biol Eng Comput* 2008;46:1161-7.
38. Crouse U, Laine-Alava MT, Warren DW. Nasal impairment in prepubertal children. *Am J Orthod Dentofacial Orthop* 2000;118:69-74.
39. Kuroi J, Modin H, Bjerkhoel A. Orthodontic maxillary expansion and its effect on nocturnal enuresis. *Angle Orthod* 1998;68:225-32.
40. Kobayashi R, Miyazaki S, Karaki M, Kobayashi E, Karaki R, Akiyama K, et al. Measurement of nasal resistance by rhinomanometry in 892 Japanese elementary school children. *Auris Nasus Larynx* 2011;38:73-6.
41. White BC, Woodside DG, Cole P. The effect of rapid maxillary expansion on nasal airway resistance. *J Otolaryngol* 1989;18:137-43.
42. Principato JJ, Wolf P. Pediatric nasal resistance. *Laryngoscope* 1985;95:1067-9.